# Diagnostic Plane Extraction from 3D Parametric Surface of the Fetal Cranium

Ana I. L. Namburete
ana.namburete@eng.ox.ac.uk
Richard V. Stebbing
richard.stebbing@eng.ox.ac.uk
J. Alison Noble
alison.noble@eng.ox.ac.uk

Biomedical Image Analysis Laboratory
Institute of Biomedical Engineering
Old Road Campus Research Building
University of Oxford
Oxford, UK

**Abstract**

In this paper, we evaluate the viability of using a 3D parametric surface model of the fetal cranium to extract diagnostic 2D ultrasound (US) image planes and biometric measurements useful in fetal growth monitoring. The parametric surface deforms to tightly delineate the inner cranial boundary, and its topology-preserving property defines a coordinate space which allows for consistent sampling of anatomical regions. Our validation experiments comparing diagnostic planes extracted from the parametric surface to those manually selected by a clinical expert demonstrate that the planes are acceptable, and biometric measurements obtained from surface-extracted planes are within clinically-acceptable error bounds (error=4.82%, $n = 191$ fetuses).

## 1 Introduction

In obstetric care, one of the main purposes of fetal brain imaging is to identify structural abnormalities. Qualitative and quantitative image data from a fetus are compared to reference standards of normal development to enable a judgement to be made about the likelihood of an abnormality being present. Biometry of the cranium is an obvious starting point for such examinations due to its echo-bright appearance on US images. Whilst not directly measuring the brain itself, cranial size is used as a proxy for this and is incorporated into most assessments of brain structure and fetal growth. During an obstetric examination, three standard axial planes are collected from the fetal brain to assess anatomic integrity (Figure 1) [1]. However, assessment of growth from these planes is complicated by inconsistencies and subjectivity in identifying the appropriate 2D diagnostic plane from the 3D brain space, which in turn affects the skull size approximation.

In this work, we propose the use of a 3D parametrization of the fetal cranial surface to extract diagnostic planes consistently from a predetermined coordinate space to which the 3D US images are aligned. Our work benefits from the surface deformation framework described in [4] in which a B-spline spherical surface is aligned to key anatomical landmarks seen in a 3D US image of the fetal brain. Using the Levenberg-Marquardt algorithm, the surface then deforms to adhere to the inner cranial boundary through a series of discrete and continuous optimization steps [3]. During the deformation process, the surface mesh

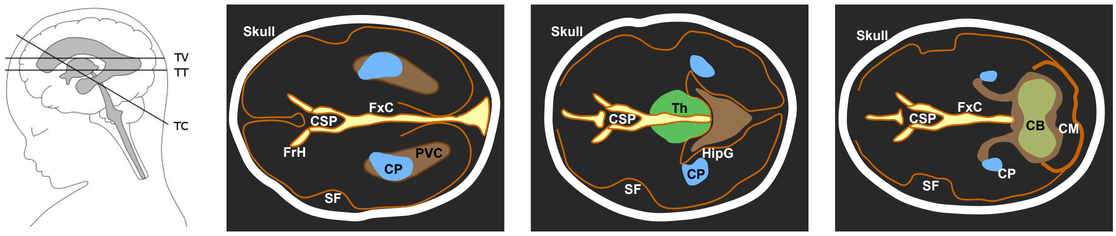


(a) Standard planes (b) TV Plane (c) TT Plane (d) TC Plane

Figure 1: **Standard Axial Planes of Fetal Head.** (a) Three axial planes used in the standard fetal neurosonography examination (from left to right): (b) transventricular (TV) plane, (c) transthalamic (TT) plane, (d) transcerebellar (TC) plane. The structures of interest in these planes are: choroid plexus (CP), posterior ventricle cavity (PVC), cavum septum pellucidum (CSP), falx cerebri (FxC), Sylvian fissure (SF), frontal horn (FrH), thalami (Th), hippocampal gyrus (HipG), cisterna magna (CM), and cerebellum (CB).

preserves topological relations between vertices, allowing for the creation of a manifold representation of the fetal skull.

The advantage of using a parametrized surface is that key points of clinical significance may be identified from which intracranial regions may be sampled and planes may be extracted on different surfaces without requiring registration between images— a challenge in fetal brain images due to underdeveloped or inconsistent neuroanatomical landmarks. In this paper, the viability of the surface at extracting the standard fetal head planes through parametrized planes whilst maintaining anatomical consistency between images of different subjects is tested, as well as the accuracy expected of the initial surface alignment provided by the user. We compare diagnostic 2D image planes selected by a clinical expert to the planes extracted from the topological surface domain, and evaluate the viability of using the surface to obtain biometric measurements useful in monitoring fetal growth.

## 2 Defining Standard Planes on Cranial Domain

The standard planes were defined on the cranial surface model (Figure 2b) based on the regions they ought to intersect on the anatomically-labelled surface (Figure 2a). A single reference brain US image was used to identify the image planes, and each diagnostic plane was defined by three cranial points selected on the Euclidean image space, $C_p \in \mathbb{R}^{3\times3}$. The points were then translated to define each standard plane on the deformed surface of the reference image, $P_j$, where $j \in \{\text{TV, TT, TC}\}$, and hence on the cranial domain.

The fetal head then underwent the surface deformation process proposed by Namburete et al. [4], and the surface points $U' \in N_U$ intersected by the standard image plane $P_j$ were used to define the standard plane $j$ on the cranial domain. Figure 2b displays the spatial definition of the standard planes on the cranial surface.

## 3 Experiments

Plane selection was performed on 52 3D US images of the fetal brain obtained from the INTERGROWTH-21$^{st}$ database, which consists of optimally healthy women with low risk of fetal abnormalities. Women included in this study ranged from $18^{+0}$ to $28^{+6}$ post-menstrual weeks' (weeks$^{+\text{days}}$) gestation. Images were collected using a Philips HD9 curvilinear probe at 2-5MHz wave frequency, and were all rendered to an isotropic voxel resolution of 0.6*mm*. 2D diagnostic planes were manually-selected from the 3D brain volumes by a clinical expert,

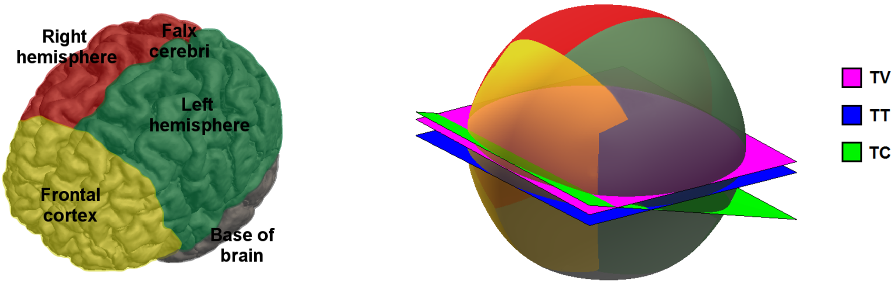


(a) Anatomical regions (b) Planes on surface domain

Figure 2: **Standard Axial Planes on Cranial Domain.** (a) Given the anatomical regions corresponding to vertices on the cranial surface model, the standard planes can be defined on the surface (b): tranventricular (TV), transthalamic (TT), and transcerebellar (TC) planes.

which were used as the ground-truth for the planes extracted from their corresponding cranial surfaces. A further experiment compared the head circumference measurements from manually-selected ($Q$) and surface-extracted ($S$) TT planes of 191 3D US images.

## 3.1 Validation of Plane Selection

The dihedral angle between the manually-selected ($Q$) and surface-extracted ($S$) clinical planes was computed as a measure of the alignment between the planes. The dihedral angle, $\theta_d(Q,S)$, is given by:

$$\theta_d(Q,S) = \arccos\left(\frac{\mathbf{n}_Q \cdot \mathbf{n}_S}{|\mathbf{n}_Q|\,|\mathbf{n}_S|}\right) \tag{1}$$

where $\mathbf{n}_Q$ and $\mathbf{n}_S$ are the normal vectors to the manually-selected and surface-extracted planes, respectively, and the norm of a vector is defined as $|\mathbf{n}| = \sqrt{n_x^2 + n_y^2 + n_z^2}$.

It should be noted, however, that although the dihedral angle is indicative of the alignment between planes, it does not translate into a clinical index. More clinically-informative indicators are: *a*) the relationship between the anatomical structures of interest visualized in the surface-extracted plane and in the manually-selected plane, and *b*) the distance between the $Q$ and $S$ planes. For instance, a good surface-extracted TC plane would demonstrate high overlap in the cerebellar region visualized in the manually-selected plane and small average distance (in mm) from the manually-selected plane. Anatomical structure overlap is an appropriate measure because the ultrasonographer selects a suitable plane from the 3D brain space on the basis of presence, shape, and size of anatomical structures of interest. The overlap between the planes was computed using the Dice Coefficient of the manual segmentations of the following anatomical structures: choroid plexus (CP), posterior ventricle cavity (PVC), cavum septum pellucidum (CSP), and cerebellum (CB). The Dice coefficient of an anatomical structure, $D_k$, is a metric indicative of plane similarity, given by

$$Dice_k = \frac{2\,|A_Q(k) \cap A_S(k)|}{|A_Q(k)| + |A_S k|} \tag{2}$$

where $k \in \{\text{CP, PVC, CSP, CB}\}$ and the $A_i(k)$ is the number of pixels of structure $k$ present in a plane $i \in \{Q,S\}$. Since the planes cannot be assumed to be parallel, it is expected that there may be a shift in the location of corresponding intracranial structures. To account for this, the intensity images were first rigidly registered and the transformation was applied to the manual segmentation images prior to computing the Dice coefficient.

The mean distance between the surface-extracted and manually-selected planes was computed by extracting the points on the cranial surface which define the contour of the skull in the surface-extracted plane and computing the average Euclidean distance between these points and the manually-extracted plane. The cranial contour points $U_Q$ are defined as the surface points which overlap with the surface-extracted plane, $U_S = (U \cap S)$, where $U \subset N_U$. The Euclidean distance between the points is defined as

$$Dist(Q,S) = \hat{\mathbf{n}}_Q \cdot U_S + p_Q \tag{3}$$

where $\hat{\mathbf{n}} = \frac{\mathbf{n}}{|\mathbf{n}|}$ is the unit normal vector, $p_Q$ is the distance of the manually-extracted plane ($Q$) from the origin, and the dot product $\hat{\mathbf{n}}_Q \cdot U_S$ represents the scalar projection of the points on the surface extracted plane ($U_S$) onto plane $Q$.

# 4 Results

The mean and standard deviation of the dihedral angles between the manually-selected and surface-extracted planes are summarized in Table 1, and Figure 3 displays visual examples of surface-extracted plane selection along with their corresponding dihedral angles. It is evident that in all image slices, the relevant anatomical structures were present in the selected planes, regardless of the dihedral angle.

The dihedral angle between $Q$ and $S$ was smallest and least variable for the TT plane: the plane containing the most anatomical landmarks as per the ISUOG guidelines [1]. In contrast, the TC plane displayed the highest variability in plane selection due to the imprecise definition of the angle of 2D image acquisition protocol and anatomical landmarks expected to be visible in the plane (Table 2). The results tabulated in Table 2 exclude 7.69% (4/52 images) of the images which were considered outliers (i.e. $|\theta_d| \geq 25°$ because image does not comply with standard acquisition protocols). These outliers constituted images satisfying any of the following criteria:

- Clinician selected an incorrect plane (due to unclear anatomy visualization caused by motion artifacts)
- Cranial surface was misaligned during the user initialization
- Intracranial structures were indiscernible

The mean Euclidean distances between $Q$ and $S$ planes were all below $5mm$ for all standard planes, which indicates that the surface-extracted planes did not greatly deviate from the planes selected by a clinician for fetal brain assessment.

Table 2 summarizes the segmentation overlap between the manually-selected and surface-extracted planes. Low Dice coefficient values are attributed to the difficulty in achieving proper alignment between non-parallel $Q$ and $S$ planes, undefined manual segmentation protocol for each anatomical structure, and the small size of the intracranial structures on each plane. However, the fact that there is overlap between the structures expected at each plane signifies that the surface-extracted planes contain the appropriate intracranial structures of relevance to clinicians. This highlights that although a surface extracted-plane may not exactly match the clinically-selected plane, it still complies with the ISUOG guidelines [1], meaning that it would be an acceptable choice of plane in a fetal neurosonography evaluation. The results also validate the parametrized surface's ability to extract planes with anatomical consistency in different subjects.

In order to assess clinical usefulness of the surface-extracted planes, we compared head circumference (HC) measurements collected from them (Figure 4a) to those obtained using the current best clinical method: the mean of three HC measurements collected from different 2D TT US scans on the same fetus (Figure 4b). The difference between the two measurements had a tight fit (i.e. RMSE=18.4$mm$, for HC ranging from 143.4$mm$ to 308.3$mm$ at $18^{+0}$ and $28^{+6}$ weeks, respectively, for our dataset), and the bias error between the two techniques was within the acceptable range of interobserver variability for HC measurements ($\pm$11.1$mm$, 4.8%), i.e. below 5% [5], suggesting clinical viability of the surface-extracted plane measurements.

Table 1: **Plane Similarity Metrics.** Mean and standard deviation values of dihedral angles between manually-selected and surface-extracted planes ($\theta_d(Q,S)$ in degrees), and mean and standard deviation distance values between the planes ($Dist(Q,S)$ in mm).

| Plane | $\theta_d(Q,S)$ | $Dist(Q,S)$ |
|---|---|---|
| TV | $1.5 \pm 8.4°$(n=50) | $4.31 \pm 1.79$ |
| TT | $0.8 \pm 6.6°$(n=51) | $3.55 \pm 1.58$ |
| TC | $2.6 \pm 7.3°$(n=48) | $4.63 \pm 1.91$ |

Table 2: **Plane Overlap Metrics.** Dice Coefficient for anatomical structures of interest ($D_k$). Blank table entries correspond to structures that were consistently absent from the plane.

| Plane | $Dice_{CP}$ | $Dice_{PVC}$ | $Dice_{CSP}$ | $Dice_{CB}$ |
|---|---|---|---|---|
| TV | $0.509 \pm 0.185$ | $0.334 \pm 0.357$ | $0.195 \pm 0.265$ | — |
| TT | $0.285 \pm 0.314$ | $0.173 \pm 0.349$ | $0.333 \pm 0.387$ | — |
| TC | — | — | $0.136 \pm 0.295$ | $0.097 \pm 0.156$ |

# 5 Conclusion

We have demonstrated the viability of using a topological manifold representation of the fetal skull to extract diagnostic image planes from which clinically-useful information can be extracted. The similarity between the surface-extracted and manually-selected planes relies on the user providing an accurate alignment of surface model and imaged brain. In this paper, we have demonstrated the ability of the parametric surface to extract diagnostic planes containing all of the key landmarks characteristic of a given plane, respecting geometric and anatomical expectations. In addition, the parametrization of the cranial surface allows for anatomical consistency in sampling images from different patients across a wide gestational age window spanning the second and early third trimesters.

Finally, we have shown that biometric measurements obtained from surface-extracted planes are within the accepted range of interobserver variability, implying that the planes would be acceptable in routine assessment of fetal growth. Further experiments include using the 3D nature of the surface model to extract measurements with potential applications to detection of craniosynostosis or craniofacial dysmorphology *in utero* [2].

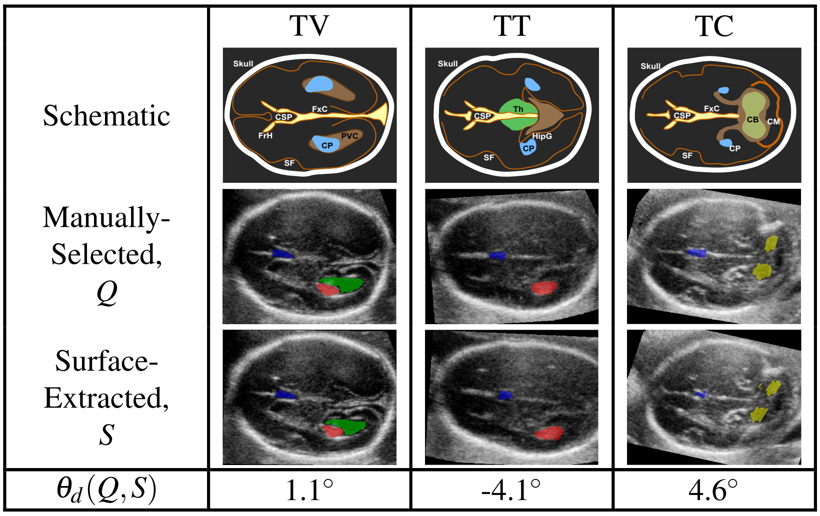


Figure 3: **TV plane selection**. Visual comparison between manually-selected (top row) and surface-extracted TV planes (bottom row) for three different subjects. Manual segmentations of anatomical landmarks are shown: choroid plexus (red), posterior ventricle cavity (green), cavum septum pellucium (blue), and cerebellum (yellow). Dihedral angle between manually-selected and surface-extracted planes is shown below each image pair.

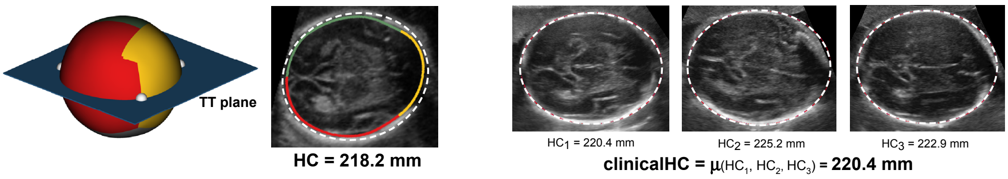


(a) Surface-extracted HC measurement (b) Clinical manual HC measurement

Figure 4: **HC measurement.** Methods of obtaining head circumference measurement from (a) surface-extracted and (b) manual-selected TT planes. For (b), HC was estimated by the mean of clinical annotations from three different images of the same subject.

# References

[1] Sonographic examination of the fetal central nervous system: guidelines for performing the ‘basic examination’ and the ‘fetal neurosonogram’. *Ultrasound Obstet Gynecol*, 29 (1):109–116, 2007.

[2] HC Chen, PY Tsai, HH Huang, HH Shih, YY Wang, CH Chang, and YN Sun. Registration-based segmentation of 3D ultrasound images for quantitative measurement of fetal craniofacial structure. *Ultrasound Med Biol*, 38(5):811–823, 2012.

[3] PE Gill, W Murray, and MH Wright. Practical optimization. 1981.

[4] AIL Namburete, RV Stebbing, and JA Noble. Cranial parametrization of the fetal head for 3D ultrasound image analysis. In *MIUA*, pages 196 – 201, 2013.

[5] I Sarris, C Ioannou, P Chamberlain, E Ohuma, F Roseman, L Hoch, DG Altman, AT Papageorghiou, and INTERGROWTH-21st. Intra- and interobserver variability in fetal ultrasound measurements. *Ultrasound Obstet Gynecol*, 39(3):266–273, 2012.